

Heat Mass Transfer Flow past an Infinite Vertical Plate with Variable Thermal Conductivity, Heat Source and Chemical Reaction

¹I. J. Uwanta, ²Murtala Sani

¹Department of Mathematics, Usmanu Danfodiyo University, Sokoto-Nigeria

²Department of Mathematics and Computer Science, Umaru Musa Yar'adua University, Katsina-Nigeria

ABSTRACT

This paper investigates the flow and heat mass transfer past an infinite vertical plate with variable thermal conductivity, heat source and chemical reaction. The non-linear, coupled partial differential equations together with the boundary conditions are reduced to dimensionless form. The resulting equations are discretized using implicit finite difference scheme of Crank-Nicolson type and solved numerically. The velocity, temperature and concentration profiles are presented graphically with tabular presentations of the Skin friction, rate of heat and mass transfer which are all computed and discussed for different values of parameters of the problem.

Keywords - Heat Transfer, Mass Transfer, Variable Thermal Conductivity, Heat Source, Vertical Plate

Date of Submission: 28 April 2014



Date of Publication: 30 May 2014

I. INTRODUCTION

The study of effects of porous boundaries on flow and heat transfer with mass transfer is important because of many engineering design applications in the field of chemical and geophysical sciences. Permeable porous plates are used in the filtration processes and also for a heated body to keep its temperature constant and to make the heat in solution of the surface more effective. The study of stellar structure on solar surface is connected with the mass transfer phenomena. Its origin is attributed to difference in temperature caused by the non-homogeneous production of heat, which in many cases can rest not only in the formation of convective currents but also in violent explosions, [1].

Most of the practical situations demand for fluids that are non-Newtonian in nature which are mainly used in many industrial and engineering applications. It is well known that a number of fluids such as molten plastic, polymeric liquid, food stuffs, etc, exhibit non-Newtonian character. The boundary layer flow of non-Newtonian fluids over a stretching sheet has been studied extensively in the recent years. [2] presented a work on flow and heat transfer in power law fluid over a stretching porous surface with variable surface temperature. Very recently, [3] considered the effects of buoyancy and variable thermal conductivity in a power law fluid past a vertical stretching sheet in the presence of non-uniform heat source.

The study of convective fluid flow with mass transfer along a vertical porous plate in the presence of magnetic field and internal heat generation is receiving considerable attention due to its useful applications in different branches of Science and Technology such as cosmical and geophysical sciences, fire engineering, combustion modeling, etc. [4] analyzed the MHD free convective flow past an accelerated vertical porous plate by finite difference method.

[5] investigated the transient free convection in cold water past an infinite vertical porous plate. [6] discussed free convection and mass transfer flow through a porous medium past an infinite vertical porous plate with time dependent temperature and concentration while [7] investigated the effect of chemical and thermal diffusion with Hall current on unsteady hydromagnetic flow near an infinite vertical porous plate and [8] reported the effects of applied magnetic field on transient convective flow in a vertical channel. [9] analyzed the effect of Hall current MHD free convection flow along an accelerated porous heated plate with mass transfer and internal heat generation. [10] studied transient free convection flow of a viscous dissipative fluid past a semi-infinite vertical plate. [11] investigated the unsteady MHD convective heat transfer past a semi-infinite vertical porous moving plate with variable suction. Also, [12] analyzed the effect of mass transfer in unsteady MHD flow and heat transfer past an infinite porous vertical moving plate while [13] discussed the unsteady free convective

flow and mass transfer of a rotating elastico - viscous liquid through porous media past a vertical porous plate and [14] studied the unsteady free convection and mass transfer boundary layer flow past an accelerated infinite vertical porous plate with suction. [15] investigated unsteady MHD free convective flow and heat transfer along a vertical porous plate with variable suction and internal heat generation. [16] obtained the analytical and numerical results for free convection flow along a porous plate with variable suction in porous medium while [17] obtained the numerical approach on parameters of the thermal radiation interaction with convection in boundary layer flow at a vertical plate with variable suction and [18] presented the convective heat and mass transfer flow over a vertical plate with Nth order chemical reaction in a porous medium.

The aim of the paper is to investigate the unsteady heat mass transfer flow past an infinite vertical plate with variable thermal conductivity and heat source in the presence of chemical reaction. The governing equations are solved numerically using the implicit finite difference scheme of Crank-Nicolson type. The effect of the parameters on the velocity, temperature and the concentration distributions of the flow fields are discussed and shown through graphs while the skin friction, rate of heat and mass transfer are discussed and shown using tables.

II. PROBLEM FORMULATION

We consider an unsteady infinite vertical isothermal porous plate of laminar natural convection flow of dissipative and radiating fluid in the presence of transverse magnetic field surrounded on one side by infinite mass of fluid like air or water and both at same temperature T'_∞ and the mass concentration C'_∞ initially. At time $t' > 0$, the plate temperature and the mass concentration is raised to T'_w and C'_w , causing the presence of temperature and concentration difference $T'_w - T'_\infty$ and $C'_w - C'_\infty$ respectively. As the plate is infinite in extent, the physical variables are functions of y' and t' where y' is taken normal to the plate and the x' -axis is taken along the plate in the vertically upward direction. It is assumed that both the variable thermal conductivity and the nth order chemical reaction are not constant. Under the Boussinesq's approximation, the governing equations in this case [19] and [20] for the flow are continuity, momentum, mass concentration and energy respectively (which is an extension of [21]):

$$\frac{\partial v'}{\partial y'} = 0 \quad (1)$$

$$\frac{\partial u'}{\partial t'} + v' \frac{\partial u'}{\partial y'} = \nu \frac{\partial^2 u'}{\partial y'^2} - \frac{\sigma B_0^2 u'}{\rho} - \frac{\nu u'}{K^*} + g\beta(T' - T'_\infty) + g\beta^*(C' - C'_\infty) - b_1^* u'^2 \quad (2)$$

$$\frac{\partial C'}{\partial t'} + v' \frac{\partial C'}{\partial y'} = D \frac{\partial^2 C'}{\partial y'^2} - R^*(C' - C'_\infty)^n \quad (3)$$

$$\frac{\partial T'}{\partial t'} + v' \frac{\partial T'}{\partial y'} = \frac{1}{\rho C_p} \frac{\partial}{\partial y'} \left(K(T') \frac{\partial T'}{\partial y'} \right) - \frac{1}{\rho C_p} \frac{\partial q_r}{\partial y'} + \frac{\nu}{C_p} \left(\frac{\partial u'}{\partial y'} \right)^2 + b^* u'^2 + \frac{Q}{\rho C_p} (T' - T'_\infty) \quad (4)$$

The initial and boundary conditions relevant to the fluid flow are:

$$\begin{aligned} t' \leq 0, \quad u' = 0, T' = T'_\infty, C' = C'_\infty & \quad \text{for all } y' \\ t' > 0, \quad u' = 0, T' = T'_w, C' = C'_w & \quad \text{at } y' = 0 \\ u' \rightarrow 0, T' \rightarrow T'_\infty, C' \rightarrow C'_\infty & \quad \text{as } y' \rightarrow \infty \end{aligned} \quad (5)$$

where ν is the kinematic viscosity of the grey fluid, σ is the Stefan-Boltzmann constant, B_0 is the constant magnetic field intensity, ρ is density, K^* is the permeability, g is the gravitational constant, β is the thermal expansion coefficient, β^* is the concentration expansion coefficient, T' is the temperature, C' is the mass concentration, D is the chemical molecular diffusivity, R^* is the chemical reaction, C_p is the specific heat at constant pressure, q_r is the radiative heat flux, u' and v' are velocity components in x and y directions respectively, t is the time, $K(T')$ is the variable thermal conductivity, b_1^* is the Forchheimer parameter of the medium, b^* is the Hall current parameter, Q is the volumetric rate of heat generation and n is the reaction order

while T'_w is the wall temperature, T'_∞ is the free stream temperature, C'_w is the species concentration at the plate surface and C'_∞ is the free stream concentration.

From the continuity equation (1), it is clear that the suction velocity is either a constant or a function of time. Hence, on integrating equation (1), the suction velocity normal to the plate is assumed in the form, $v' = -v_0$ where v_0 is a scale of suction velocity which is non-zero positive constant. The negative sign indicates that the suction is towards the plate and $v_0 > 0$ corresponds to steady suction velocity normal at the surface.

Assuming the radiative heat flux from the Rosseland approximation to have the form:

$$\frac{\partial q_r}{\partial y'} = -4\sigma a^* (T'^4_\infty - T'^4) \quad (6)$$

σ is the Stefan-Boltzmann constant, a^* is the mean absorption effect for thermal radiation constant. We assume that the temperature differences within the flow are sufficiently small such that T'^4 can be expanded in a Taylor series about T'_∞ and neglecting higher order terms give:

$$T'^4 \cong 4T'T'^3_\infty - 3T'^4_\infty \quad (7)$$

The variable thermal conductivity depends on temperature. It is used by [22], as follows:

$$K(T') = k_0 \{1 + \gamma(T' - T'_\infty)\} \quad (8)$$

where k_0 is the thermal conductivity of the ambient fluid and γ is a constant.

III. METHOD OF SOLUTION

To solve the governing equations in dimensionless form, we introduce the following non-dimensional quantities:

$$U = \frac{u'}{U_0}, y = \frac{y'U_0}{\nu}, t = \frac{t'U_0^2}{\nu}, \theta = \frac{T' - T'_\infty}{T'_w - T'_\infty}, C = \frac{C' - C'_\infty}{C'_w - C'_\infty}, \tau = \gamma(T'_w - T'_\infty), b = \frac{b^* \nu}{(T'_w - T'_\infty)},$$

$$Sc = \frac{\nu}{D}, Pr = \frac{\nu \rho c_p}{k_0}, Ec = \frac{U_0^2}{c_p (T'_w - T'_\infty)}, Gr = \frac{g \beta \nu (T'_w - T'_\infty)}{U_0^3}, Gc = \frac{g \beta^* \nu (C'_w - C'_\infty)}{U_0^3}, \alpha = \frac{\nu_0}{U_0}, \quad (9)$$

$$K = \frac{K^* U_0^2}{\nu}, N = \frac{16a\sigma^* T'^3_\infty \nu}{k_0 U_0}, M = \frac{\nu \sigma B_0^2}{\rho U_0^2}, Kr = \frac{\nu R^* (C'_w - C'_\infty)^{n-1}}{U_0^2}, b_1 = \frac{b_1^* \nu}{U_0}, S = \frac{Q \nu^2}{k_0 U_0^2}$$

The governing equations on using (9) into (1), (2), (3), (5) and (6) to (9) into (4) reduce to the following:

$$\frac{\partial U}{\partial t} - \alpha \frac{\partial U}{\partial y} = \frac{\partial U}{\partial y^2} - \left(M + \frac{1}{K} \right) U + Gr\theta + GcC - b_1 U^2 \quad (10)$$

$$\frac{\partial C}{\partial t} - \alpha \frac{\partial C}{\partial y} = \frac{1}{Sc} \frac{\partial^2 C}{\partial y^2} - KrC^n \quad (11)$$

$$\frac{\partial \theta}{\partial t} - \alpha \frac{\partial \theta}{\partial y} = \frac{(1 + \tau\theta)}{Pr} \frac{\partial^2 \theta}{\partial y^2} + \frac{\tau}{Pr} \left(\frac{\partial \theta}{\partial y} \right)^2 + \frac{(S - N)}{Pr} \theta + Ec \left(\frac{\partial U}{\partial y} \right)^2 + bU^2 \quad (12)$$

subject to the boundary conditions

$$\begin{aligned} t \leq 0, \quad U = 0, \theta = 0, C = 0 & \quad \text{for all } y \\ t > 0, \quad U = 0, \theta = 1, C = 1 & \quad \text{at } y = 0 \\ U \rightarrow 0, \theta \rightarrow 0, C \rightarrow 0 & \quad \text{as } y \rightarrow \infty \end{aligned} \quad (13)$$

where Pr is the Prandtl number, Sc is Schmidt number, Ec is Eckert number, Gr is thermal Grashof number, Gc is mass Grashof number, b_1 is the inertia number, and M is magnetic field, K is porosity, N is the radiation, α is suction, τ is the variable thermal conductivity, Kr is the chemical reaction, b is Hall current and S is heat source parameters.

IV. NUMERICAL PROCEDURE

In order to solve the unsteady, non-linear, coupled equations (10) to (12) under the boundary condition (13), an implicit finite difference scheme of the Crank-Nicolson type has been employed. The finite difference equations corresponding to equations (10) to (13) are as follows:

$$-r_1 U_{i-1}^{j+1} + (1 + 2r_1) U_i^{j+1} - r_1 U_{i+1}^{j+1} = r_2 U_{i-1}^j + (1 - 2r_2 - \gamma r_3 - r_4) U_i^j + (r_2 + \gamma r_3) U_{i+1}^j + \Delta t Gr \theta_i^j + \Delta t Gc C_i^j - \Delta t b_1 (U_i^j)^2 \quad (14)$$

$$-r_1 C_{i-1}^{j+1} + (Sc + 2r_1) C_i^{j+1} - r_1 C_{i+1}^{j+1} = r_2 C_{i-1}^j + (Sc - 2r_2 - \gamma r_3 Sc) C_i^j + (r_2 + \gamma r_3 Sc) C_{i+1}^j - Kr Sc \Delta t (C_i^j)^n \quad (15)$$

$$-qr_1 \theta_{i-1}^{j+1} + (Pr + 2qr_1) \theta_i^{j+1} - qr_1 \theta_{i+1}^{j+1} = qr_2 \theta_{i-1}^j + (Pr - 2qr_2 - \gamma r_3 Pr - N \Delta t + S \Delta t) \theta_i^j + (qr_2 + \gamma r_3 Pr) \theta_{i+1}^j + \tau r_5 (\theta_{i+1}^j - \theta_{i-1}^j)^2 + Pr Ec r_5 (U_{i+1}^j - U_{i-1}^j)^2 + Pr \Delta t b (U_i^j)^2 \quad (16)$$

$$U_{i,j} = 0, \theta_{i,j} = 0, C_{i,j} = 0$$

$$U_{0,j} = 0, \theta_{0,j} = 1, C_{0,j} = 1 \quad (17)$$

$$U_{m,j} \rightarrow 0, \theta_{m,j} \rightarrow 0, C_{m,j} \rightarrow 0$$

where $r_1 = \frac{\alpha \Delta t}{(\Delta y)^2}$, $r_2 = \frac{(1 - \alpha) \Delta t}{(\Delta y)^2}$, $r_3 = \frac{\Delta t}{\Delta y}$, $r_4 = \Delta t \left(M + \frac{1}{K} \right)$, $r_5 = \frac{\Delta t}{4(\Delta y)^2}$, $q = 1 + \tau \theta_1^j$ and m

corresponds to ∞ .

The mesh sizes along y - direction and time t -direction are Δy and Δt respectively while the index i refers to space y and j refers to time t . The finite difference equations (14) - (16) at every internal nodal point on a particular n -level constitute a tridiagonal system of equations which are solved by using the Thomas Algorithm.

In each time step, the concentration and temperature profiles have been computed first from equations (15) and (16) and then the computed values are used to obtain the velocity profile which meets the convergence criteria.

The skin friction coefficient, rate of heat and mass transfer in terms of Nusselt number and Sherwood number respectively are given by

$$C_f = \left(\frac{\partial U}{\partial y} \right)_{y=0}, \quad Nu = \left(\frac{\partial \theta}{\partial y} \right)_{y=0}, \quad Sh = \left(\frac{\partial C}{\partial y} \right)_{y=0}$$

V. RESULTS AND DISCUSSION

The numerical solutions are simulated for different values of the Prandtl number (Pr), Schmidt number (Sc), Eckert number (Ec), thermal Grashof number (Gr), mass Grashof number (Gc), Inertia number (b_1), radiation (N), magnetic field (M), porosity (K), variable thermal conductivity (τ), suction (α), reaction order (n), chemical reaction (Kr), Hall current (b) and heat source (S) parameters. The following parameters values are fixed throughout the calculations except where otherwise stated, Pr = 0.71, Sc = 0.62, Ec = 0.01, M = 1.0, K = 1.0, Gr = 1.0, Gc = 1.0, N = 0.1, $b_1 = 1.0$, b = 1.0, S = 1.0, $\alpha = 1.0$, $\tau = 0.1$, Kr = 0.1, n = 1.0.

The velocity profiles are illustrated in Figures 1 to 12 for different values of Prandtl number (Pr = 0.71, 1.0, 3.0, 7.0), Schmidt number (Sc = 0.22, 0.62, 0.78, 2.63), thermal Grashof number (Gr = 1, 5, 10, 15), mass Grashof number (Gc = 1, 5, 10, 15), Inertia number ($b_1 = 1, 10, 20, 30$), magnetic field (M = 1, 5, 10, 15), porosity (K = 0.1, 0.5, 1.0, 1.5), radiation (N = 1, 5, 10, 15), suction ($\alpha = 2, 4, 6, 8$), variable thermal conductivity ($\tau = 0.1, 0.5, 1.0, 1.5$), chemical reaction (Kr = 0.1, 1.0, 10, 100) and heat source (S = 3, 5, 7, 9) parameters.

In Figure 1, it is seen that the velocity decrease with increasing Prandtl number also Figure 2 reveals that, the velocity decrease with increase in the Schmidt number and likewise, Figure 3 shows that, the velocity decreases with increase in the magnetic field parameter. But, Figure 4 indicates that, the velocity increase whenever porosity parameter increases also Figure 5 represents the thermal Grashof number and it is observed that, the velocity increase with increasing thermal Grashof number just like Figure 6 which reveals that, the velocity increase when the mass Grashof number increased. While from Figure 7, it shows that, the velocity decrease with increasing radiation parameter and similarly for the suction parameter, Figure 8 indicates that, the velocity decrease with increase in the suction parameter. In Figure 9, it is seen that, the velocity increase with increasing variable thermal conductivity parameter whereas in Figure 10 we found that, the velocity decrease when the chemical reaction parameter increase just as in Figure 11 where the velocity decreases with increasing Inertia number. Figure 12 indicates that, the velocity increase whenever the heat source is increased.

The concentration profiles are illustrated in Figures 13 to 15 for different values of Schmidt number ($Sc = 0.22, 0.62, 0.78, 2.63$), suction ($\alpha = 2, 4, 6, 8$) and chemical reaction ($Kr = 10, 30, 50, 70$) parameter as in Figures 13, 14, and 15 respectively.

In Figure 13, it is noticed that, the concentration decrease with increase in the Schmidt number and likewise Figure 14 reveals that, the concentration decrease with increase in the suction parameter. Similarly, Figure 15 indicates that, the concentration decrease whenever the chemical reaction parameter increased.

The temperature profiles have been studied and presented in Figures 16 to 20 for different values of Prandtl number ($Pr = 0.71, 1.0, 3.0, 7.0$), radiation ($N = 1, 5, 10, 15$), suction ($\alpha = 2, 4, 6, 8$), variable thermal conductivity ($\tau = 0.1, 0.5, 1.0, 1.5$) and heat source ($S = 3, 5, 7, 9$) parameters shown in Figures 16, 17, 18, 19 and 20 respectively.

In Figure 16, it is observed that, the temperature decrease with increase in the Prandtl number. Also, Figure 17 reveals that the temperature decrease with increase of the radiation parameter and similarly for the suction parameter, Figure 18 indicates that, the temperature decrease whenever the suction parameter increased. Figure 19 shows that, the temperature increase with increase of the variable thermal conductivity parameter and similarly for Figure 20, the temperature increase with respect to increase in the heat source parameter.

Tables 1 to 3 are the tables for Skin friction, Nusselt number and Sherwood number for the numerical solution.

The Skin friction is illustrated in Table 1 for different values of Prandtl number Pr , thermal Grashof number Gr , mass Grashof number Gc , Schmidt number, chemical reaction Kr , suction α , magnetic field M , radiation N and S heat source parameters. In the Table, it is observed that increase in the Prandtl number, Schmidt number, chemical reaction, suction, magnetic field and radiation parameters leads to decrease in the Skin friction while the Skin friction increases whenever the thermal Grashof number, mass Grashof number and heat source parameter increases.

The Nusselt number is presented in Table 2 for different values of Prandtl number Pr , thermal Grashof number Gr , radiation N , Hall current b and α suction parameters. From the Table, it is noticed that the Nusselt number increase with increasing Prandtl number, radiation and suction parameters but increasing the thermal Grashof number and Hall current parameter results to decrease of the Nusselt number.

Similarly, the Sherwood number is demonstrated in Table 3 for different values of Schmidt number Sc , chemical reaction Kr and α suction parameters. Results from the Table shows that the Sherwood number increases whenever the Schmidt number, chemical reaction and suction parameters increase.

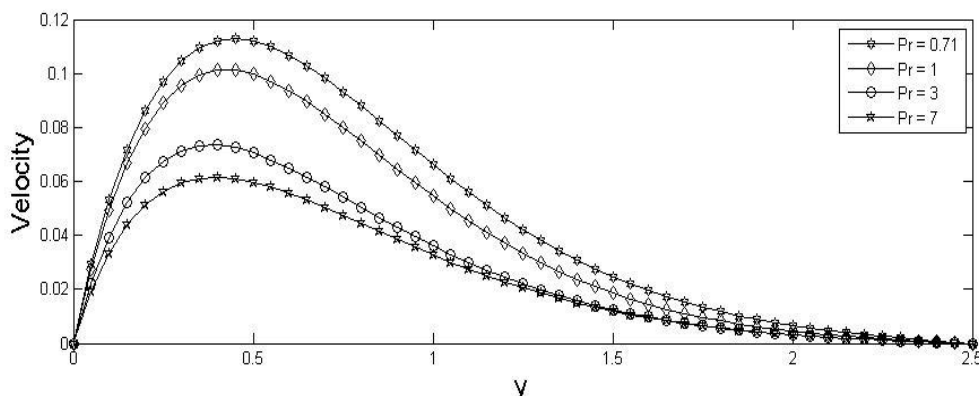


Figure 1: Variation of Velocity against y for different values of Pr .

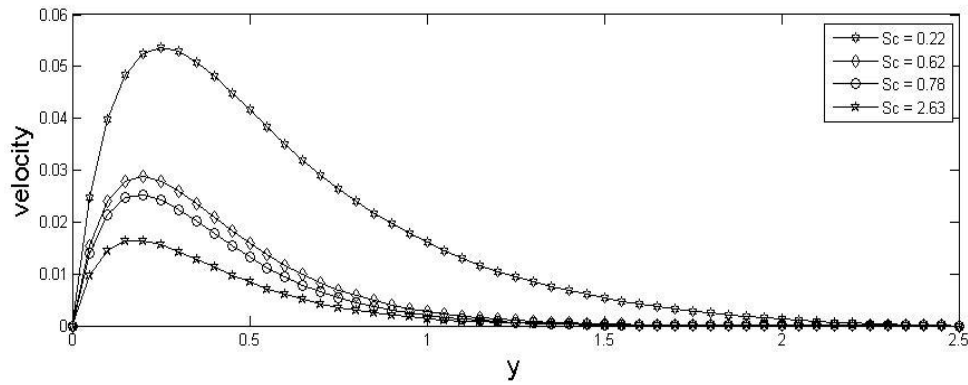


Figure 2: Variation of Velocity against y for different values of Sc.

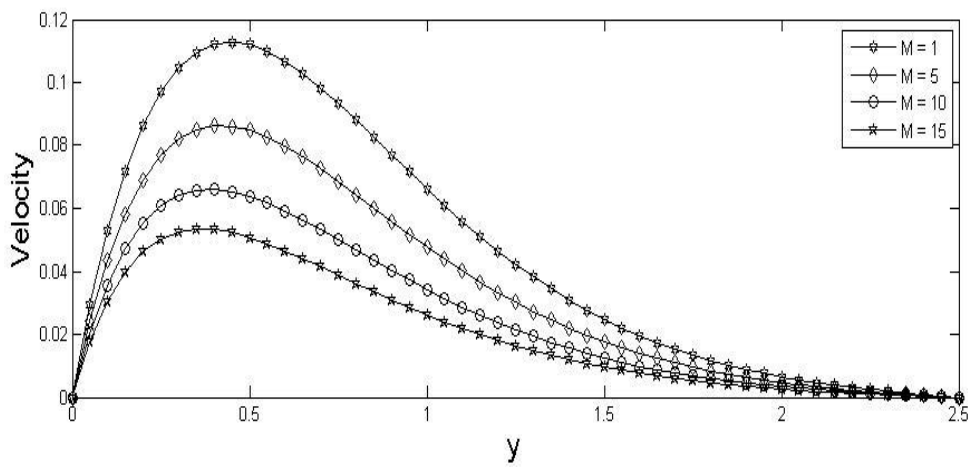


Figure 3: Variation of Velocity against y for different values of M.

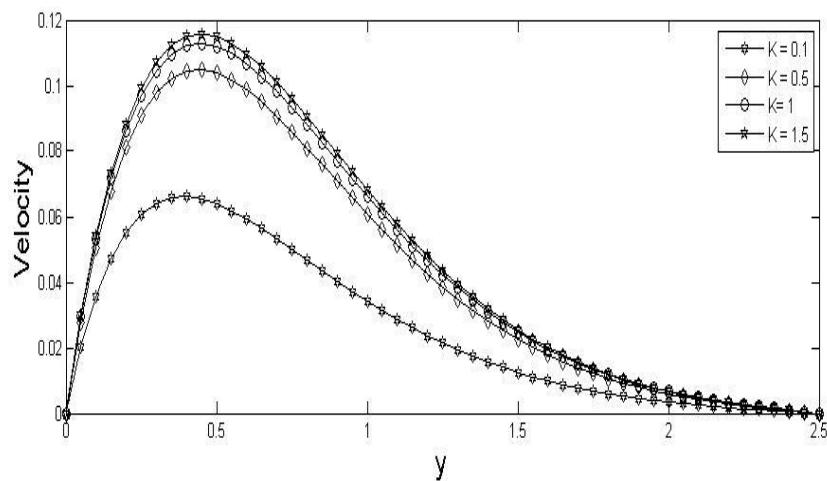


Figure 4: Variation of Velocity against y for different values of K.

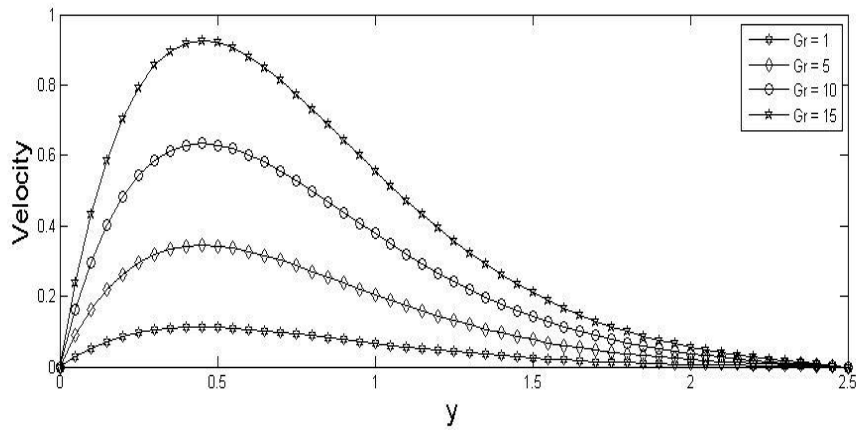


Figure 5: Variation of Velocity against y for different values of Gr.

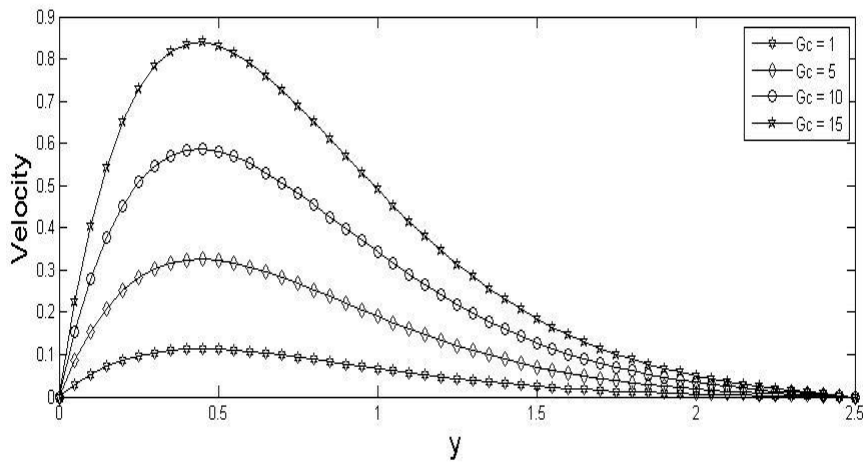


Figure 6: Variation of Velocity against y for different values of Gc.

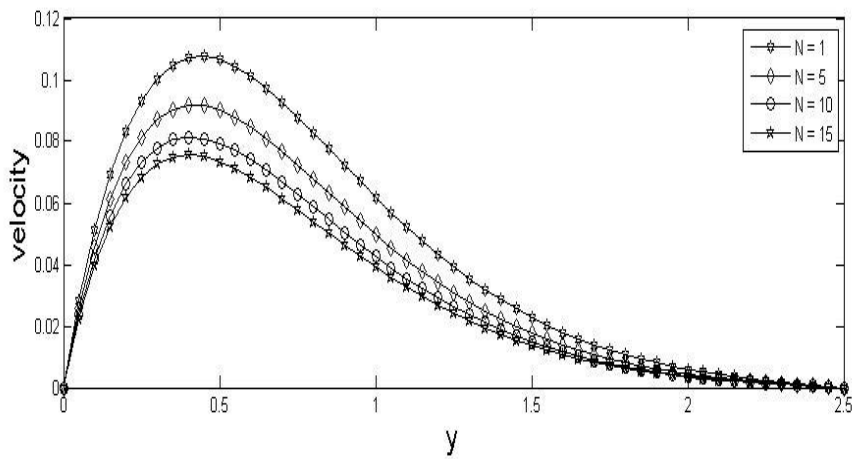


Figure 7: Variation of Velocity against y for different values of N.

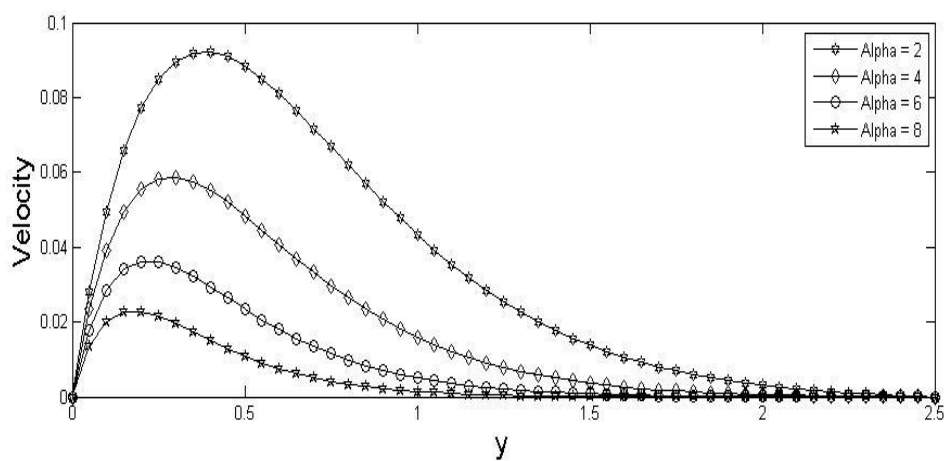


Figure 8: Variation of Velocity against y for different values of α .

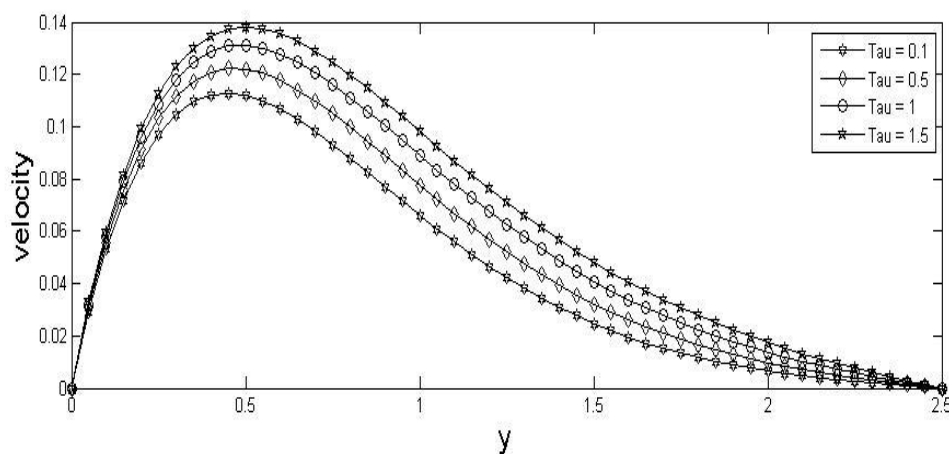


Figure 9: Variation of Velocity against y for different values of τ .

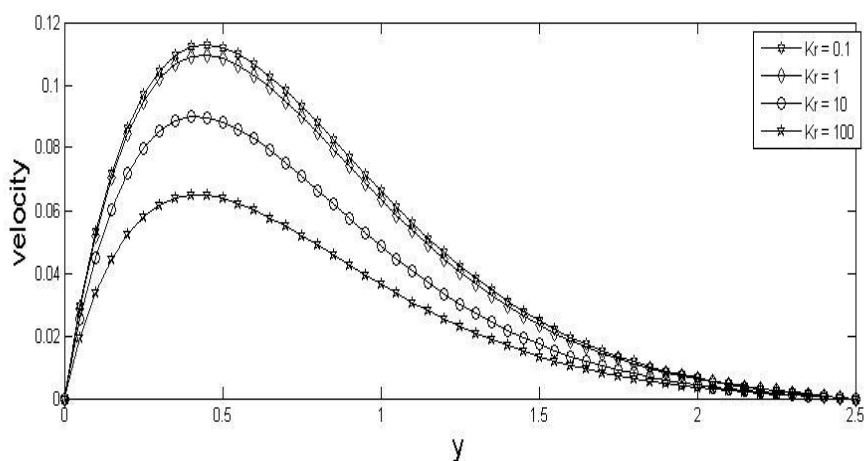


Figure 10: Variation of Velocity against y for different values of Kr.

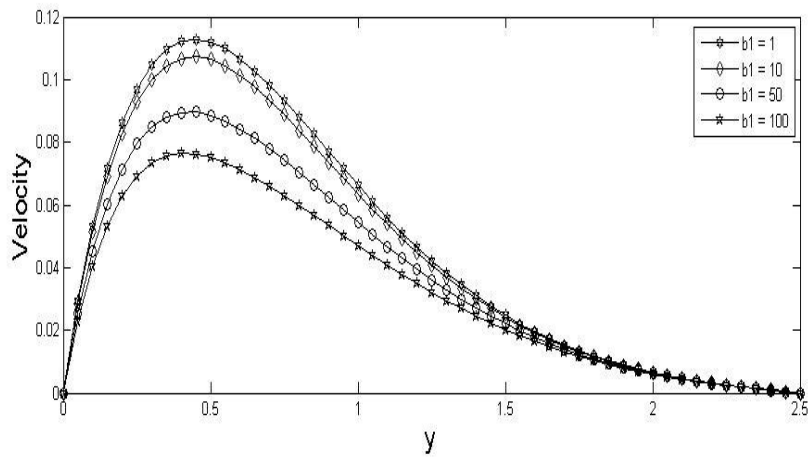


Figure 11: Variation of Velocity against y for different values of b_1 .

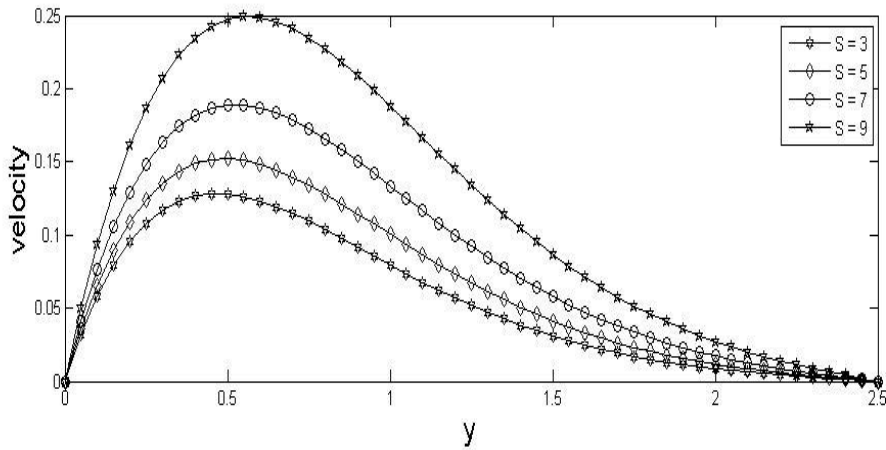


Figure 12: Variation of Velocity against y for different values of S.

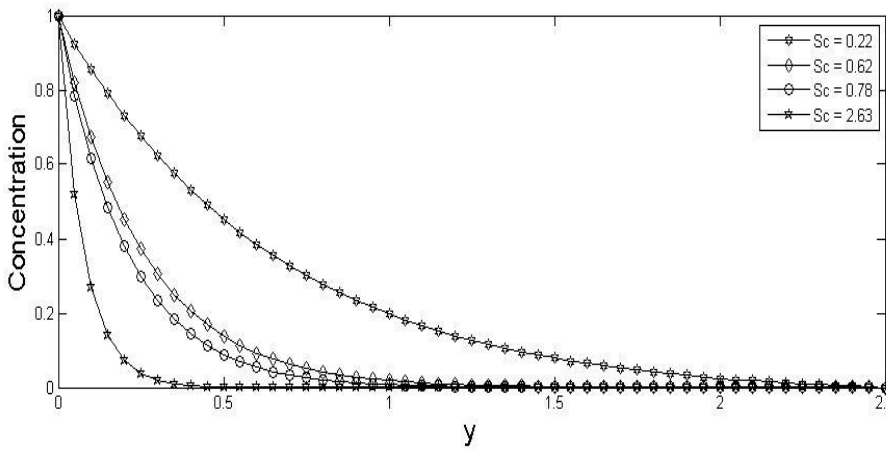


Figure 13: Variation of Concentration against y for different values of Sc .

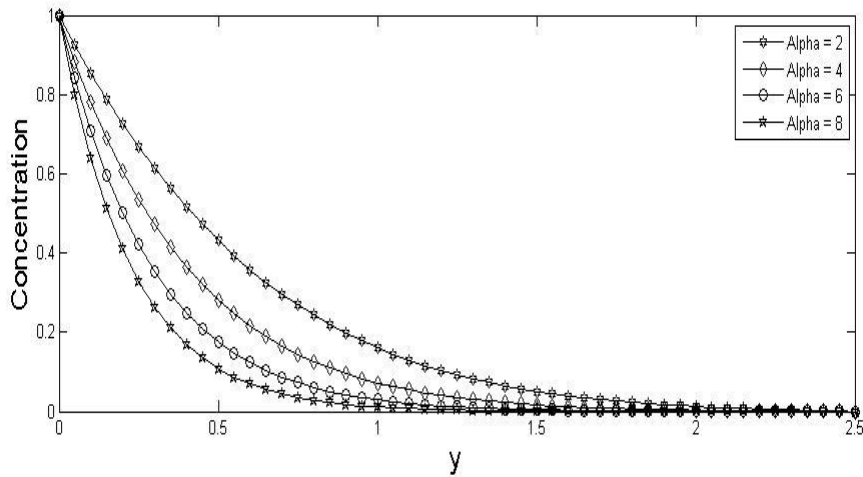


Figure 14: Variation of Concentration against y for different values of α .

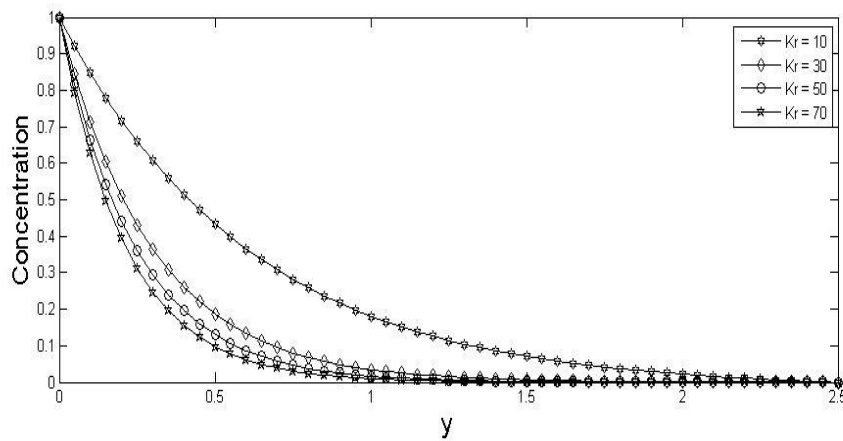


Figure 15: Variation of Concentration against y for different values of Kr .

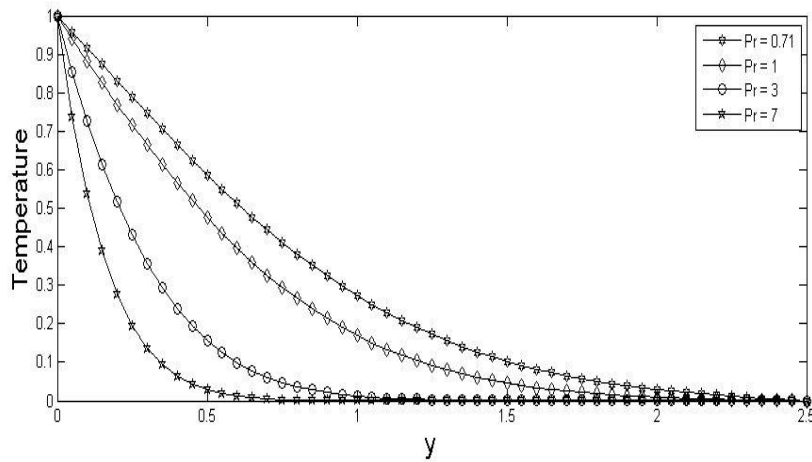


Figure 16: Variation of Temperature against y for different values of Pr .

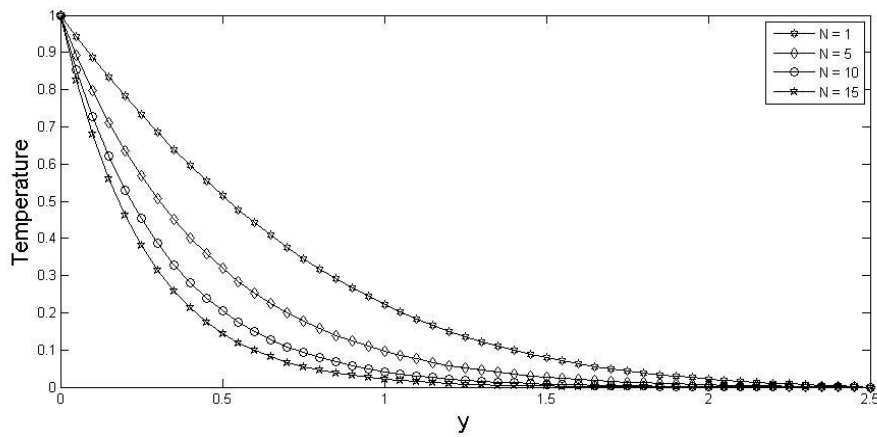


Figure 17: Variation of Temperature against y for different values of N.

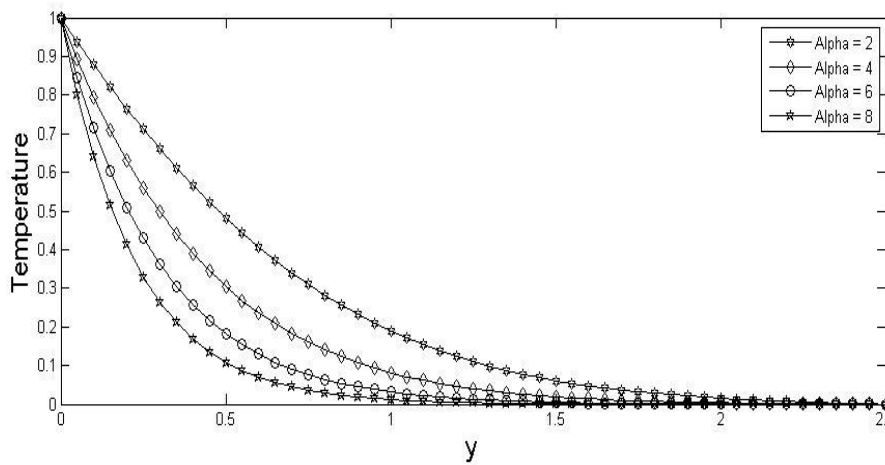


Figure 18: Variation of Temperature against y for different values of α .

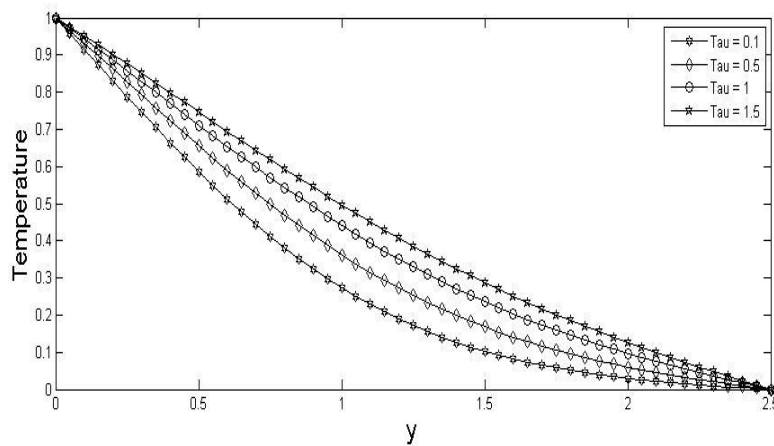


Figure 19: Variation of Temperature against y for different values of τ .

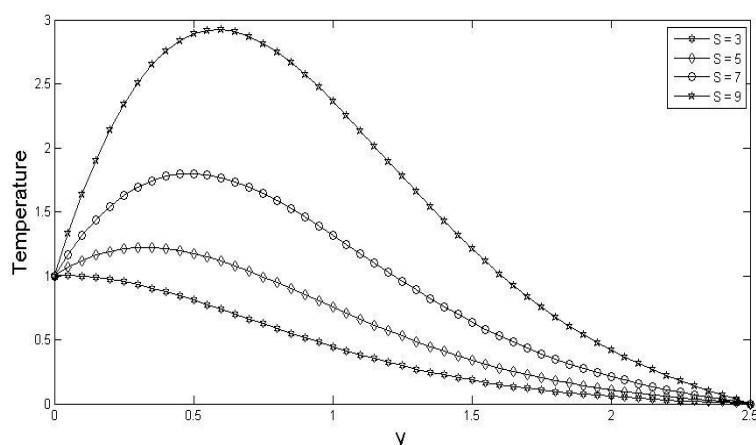


Figure 20: Variation of Temperature against y for different values of S.

TABLE 1: Skin friction for different values of Pr, Gr, Gc, Sc, Kr, α , M, N and S.

Pr	Gr	Gc	Sc	Kr	α	M	N	S	C_f
0.71	1	1	0.62	0.1	1	1	0.1	1	0.6439
1	1	1	0.62	0.1	1	1	0.1	1	0.6058
0.71	5	1	0.62	0.1	1	1	0.1	1	1.9552
0.71	1	5	0.62	0.1	1	1	0.1	1	1.8857
0.71	1	1	0.78	0.1	1	1	0.1	1	0.6227
0.71	1	1	0.62	1	1	1	0.1	1	0.6320
0.71	1	1	0.62	0.1	4	1	0.1	1	0.5407
0.71	1	1	0.62	0.1	1	5	0.1	1	0.5399
0.71	1	1	0.62	0.1	1	1	1	1	0.6249
0.71	1	1	0.62	0.1	1	1	0.1	3	0.6979

TABLE 2: Nusselt number for different values of Pr, Gr, N, b and α .

Pr	Gr	N	b	α	Nu
0.71	1	0.1	1	1	0.8356
1	1	0.1	1	1	1.1964
0.71	5	0.1	1	1	0.8180
0.71	1	1	1	1	1.1653
0.71	1	0.1	10	1	0.8163
0.71	1	0.1	1	4	2.2608

TABLE 3: Sherwood number for different values of Sc, Kr and α .

Sc	Kr	α	Sh
0.62	0.1	1	1.1604
0.78	0.1	1	1.3499
0.62	1	1	1.3640
0.62	0.1	4	2.4522

VI. CONCLUSION

The paper presents the heat mass transfer flow past an infinite vertical plate with variable thermal conductivity, heat source and chemical reaction. The dimensionless governing equations are non-dimensionalized and then solved numerically using the implicit finite difference scheme of Crank-Nicolson type. Numerical solutions are presented for the fluid flow and heat mass transfer characteristics for different values of parameters involved in the problem. The present study will serve as a scientific tool for understanding more complex flow problems concerning with the various physical parameters.

The conclusion shows that:

- ❖ The velocity increase with increase in the thermal Grashof number, mass Grashof number, variable thermal conductivity, porosity and heat source parameters whereas the velocity decrease with increasing Prandtl number, Schmidt number, Inertia number, magnetic field, radiation, suction and chemical reaction parameters.

- ❖ The temperature increase with increase in variable thermal conductivity and heat source parameters while the temperature decrease with increasing Prandtl number, radiation and suction parameters.
- ❖ The concentration decrease with increase in Schmidt number, suction and chemical reaction parameters.

REFERENCES

- [1] K. Rachna, Unsteady MHD flow, heat and mass transfer along an accelerated vertical porous plate in the influence of viscous dissipation, heat source and variable suction, *International Journal of Mathematics and Computer Applications Research*, 3(1), 2013, 229-236.
- [2] I. A. Hassanein, A. A. Abdullah and R. S. R. Gorla, Flow and heat transfer in a power law fluid over a non-isothermal stretching sheet, *Mathematics and Computational Model*, 28, 1998, 105-116.
- [3] M. S. Abel and N. Mahesha, Effects of thermal buoyancy and variable thermal conductivity in a power law fluid past a vertical stretching sheet in the presence of non uniform heat source, *International Journal of Nonlinear Mechanics*, 44, 2009, 1-12.
- [4] A. K. Singh, Finite difference analysis of MHD free convective past an accelerated vertical porous plate, *Astrophysics Space Science*, 248, 1983, 395-400.
- [5] A. K. Singh and V. M. Soundalgekar, Transient free convection in cold water past an infinite vertical porous plate, *International Journal of Energy Research*, 14, 1990, 413-420.
- [6] M. A. Sattar, Free convection and mass transfer flow through a porous medium past an infinite vertical porous plate with time dependent temperature and concentration, *International Journal of Pure and Applied Mathematics*, 23, 1994, 759-766.
- [7] M. Acharya, G. C. Dash and L. P. Singh, Effect of chemical and thermal diffusion with Hall current on unsteady hydromagnetic flow near an infinite vertical porous plate, *Journal of Applied Physics*, 28, 1995, 2455-2464.
- [8] B. K. Jha, Effects of applied magnetic field on transient free convective flow in a vertical channel, *Indian Journal of Pure and Applied Mathematics*, 29, 1998, 441-445.
- [9] G. C. Dash and S. S. Das, Hall effect on MHD flow along an accelerated porous flat plate with mass transfer and internal heat generation, *Mathematical Engineering*, 7(4), 1999, 389-404.
- [10] V. M. Soundalgekar, B. S. Jaisawal, A. G. Uplekar and H. S. Takhar, Transient free convection flow of a viscous dissipative fluid past a semi-infinite vertical plate, *Journal of Applied Mechanics and Engineering*, 4, 1999, 203-218.
- [11] Y. J. Kim, Unsteady MHD convective heat transfer past a semi-infinite vertical porous moving plate with variable suction, *International Journal of Engineering Science*, 38, 2000, 833-845.
- [12] P. R. Sharma and U. Mishra, Effect of mass transfer in unsteady MHD flow and heat transfer past an infinite porous vertical moving plate, *Indian Journal of Theoretical Physics*, 50, 2002, 109-115.
- [13] J. P. Panda, G. C. Dash and S. S. Das, Unsteady free convective flow and mass transfer of a rotating elasticoviscous liquid through porous media past a vertical porous plate, *Applied Mathematical Sciences and Engineering Journal*, 72(3), 2003, 47-59.
- [14] S. S. Das, S. K. Sahoo and G. C. Dash, Numerical solution of mass transfer effects on unsteady flow past an accelerated vertical porous plate with suction, *Bulletin of Malaysian Mathematical Science Society*, 29(2), 2006, 33-42.
- [15] P. R. Sharma and G. Singh, Unsteady MHD free convective flow and heat transfer along a vertical porous plate with variable suction and internal heat generation, *International Journal of Applied Mathematics and Mechanics*, 4, 2008, 1-8.
- [16] M. A. Sattar, M. M. Rahman and M. M. Alam, Free convection flow and heat transfer through a porous vertical plate immersed in a porous medium with variable suction, *Journal of Energy, Heat and Mass Transfer*, 21, 2000, 17-21.
- [17] M. Ferdows, M. A. Sattar and M. N. A. Siddiki, Numerical approach on parameters of the thermal radiation interaction with convection in boundary layer flow at a vertical plate with variable suction, *Thammasat International Journal of Science and Technology*, 9, 2004, 19-28.
- [18] I. J. Uwanta and U. Halima, Convective heat and mass transfer flow over a vertical plate with Nth order chemical reaction in a porous medium, *International Journal of Scientific Engineering and technology*, 3(2), 2014, 172-185.
- [19] P. K. Sharma, Influence of periodic temperature and concentration on unsteady free convective viscous incompressible flow and heat transfer past a vertical plate in slip flow regime, *Mathematica XIII*(1), 2005, 51-62.
- [20] A. Sahin, Influence of chemical reaction on transient MHD free convection flow over a vertical plate in slip-flow regime, *Emirates Journal for Engineering Research*, 15(1), 2010, 25-34.
- [21] S. D. Moses and H. A. Funmilayo, Dissipation, MHD and radiation in a Darcy-Forcheimer porous medium, *Journal of Mathematics Research*, 4(2), 2012, 110-114.